

---

## REVIEW

# Prostate cancer PET tracers: essentials for the urologist

Tyler J. Fraum, MD,<sup>1</sup> Daniel R. Ludwig, MD,<sup>1</sup> Eric H. Kim, MD,<sup>2</sup>  
Paul Schroeder, BS,<sup>3</sup> Thomas A. Hope, MD,<sup>4</sup> Joseph E. Ippolito, MD<sup>1</sup>

<sup>1</sup>Mallinckrodt Institute of Radiology, Washington University School of Medicine, St. Louis, Missouri, USA

<sup>2</sup>Department of Urology, Washington University School of Medicine, St. Louis, Missouri, USA

<sup>3</sup>Saint Louis University School of Medicine, St. Louis, Missouri, USA

<sup>4</sup>Department of Radiology, University of California at San Francisco, San Francisco, California, USA

---

FRAUM TJ, LUDWIG DR, KIM EH, SCHROEDER P, HOPE TA, IPPOLITO JE. Prostate cancer PET tracers: essentials for the urologist. *Can J Urol* 2018;25(4): 9371-9383.

**Introduction:** In the past, positron emission tomography (PET) has played a relatively limited role in prostate cancer imaging. However, in recent years, several new PET tracers have emerged, offering potential improvements in diagnostic performance for both the detection of prostate cancer metastases at initial staging and the localization of recurrent disease.

**Materials and methods:** We reviewed the literature for prostate cancer PET tracers that are either being used for patient management or being evaluated in clinical research trials. For each tracer, we compiled clinically relevant background information and evidence supporting clinical

use, with the intention of providing a high-yield primer for urologists managing patients with prostate cancer.

**Results:** <sup>18</sup>F-FDG, <sup>18</sup>F-NaF, <sup>11</sup>C-choline, and <sup>18</sup>F-fluciclovine have all proven useful for prostate cancer imaging, though the utility of each of these tracers is limited to targeted management questions and particular clinical settings. In contrast, the newer prostate-specific membrane antigen (PSMA) agents may prove useful as general purpose PET tracers for prostate cancer imaging. Numerous other novel PET tracers have shown promising results in pre-clinical studies.

**Conclusion:** Basic knowledge of these PET tracers, specifically their strengths, weaknesses, and indications for use, is essential to urologists and other physicians caring for patients with prostate cancer.

**Key Words:** PET tracers, prostate cancer, imaging, positron emission tomography

---

## Introduction

Positron emission tomography (PET) has become the standard-of-care for the initial staging and subsequent treatment response assessment of many different malignancies. Although [<sup>18</sup>F]-fluorodeoxyglucose (<sup>18</sup>F-FDG) is the workhorse tracer for the vast majority of oncologic PET applications, it currently has a limited role in prostate cancer imaging. Consequently, there is a considerable clinical need for alternative PET tracers with better performance for initial staging and localizing sites of disease in patients with biochemical recurrence (BCR). Furthermore, such PET tracers may have the ability to interrogate the biological pathways

underlying prostate cancer behavior, potentially influencing selection of treatment regimens.

Here, we provide a comprehensive review of PET tracers that are either currently available or under active investigation as prostate cancer imaging agents. We first describe the PET tracers that are already approved by the United States Food and Drug Administration (FDA). Next, we discuss the promising class of tracers that target the prostate-specific membrane antigen (PSMA). Finally, we briefly cover several new classes of PET tracers that are currently in the development pipeline. Overall, knowledge of these PET tracers, specifically their strengths, weaknesses, and indications for use, is essential to urologists and other physicians caring for patients with prostate cancer.

## FDA-approved tracers

Targeting mechanisms, imaging indications, and strengths/weaknesses of the FDA-approved tracers, as well as relevant prostate-specific antigen (PSA) values, are summarized in Table 1.

---

Accepted for publication July 2018

Address correspondence to Dr. Joseph E. Ippolito, Washington University School of Medicine, 510 S. Kingshighway Blvd., Box 8131, St. Louis, MO 63110 USA

<sup>18</sup>F-FDG

*Background*

<sup>18</sup>F-FDG is a radiolabeled analogue of glucose that is enzymatically trapped within cells in proportion to the rate of aerobic glycolysis. Because cancer cells generally utilize this metabolic pathway to a greater extent than non-cancer cells (the Warburg effect), <sup>18</sup>F-FDG preferentially localizes to malignant tumors relative to non-malignant tissues.<sup>1</sup> The main sites of physiologic <sup>18</sup>F-FDG activity (in patients that are appropriately fasting prior to administration) are the brain, tonsils, vocal cords, myocardium, liver, spleen,

bowel, renal pelvis, ureters, and urinary bladder.<sup>2</sup> Currently, <sup>18</sup>F-FDG-PET is FDA-approved for patients with histologically established diagnoses of cancer and for patients in whom cancer is strongly suspected on the basis of a different imaging study or other diagnostic test. However, for prostate cancer, the Center for Medicare & Medicaid Services covers <sup>18</sup>F-FDG-PET only for subsequent treatment strategy guidance (i.e., initial treatment strategy indications are not reimbursed).<sup>3</sup>

*Evidence supporting clinical use*

Some of the earliest studies of <sup>18</sup>F-FDG-PET for prostate cancer reported disappointing results, giving rise to

TABLE 1. FDA-approved PET tracers used in prostate cancer imaging

PET tracer	Mechanism of targeting	Imaging indications	Strengths	Weaknesses	Relevant PSA ranges
<sup>18</sup> F-FDG	Preferential uptake into malignant cells due to upregulated aerobic glycolysis	Staging of high risk disease when other tracers are not available	Widely available; potential prognostic value	Poor sensitivity for both initial staging and recurrence localization	Positive scans in BCR <sup>8</sup> PSA ≤ 2 ng/mL: 0/10 (0%) 2 < PSA ≤ 4 ng/mL: 1/9 (11%) 4 < PSA ≤ 10 ng/mL: 1/10 (10%) > 10 ng/mL: 1/8 (13%)
<sup>18</sup> F-NaF	Incorporation into matrix of abnormal bone more than normal bone	Evaluation of known or suspected osseous metastatic disease	Superior to conventional bone scans in speed, spatial resolution, and diagnostic accuracy	Tedious interpretation due to tracer uptake by numerous benign processes	Positive scans in BCR <sup>8</sup> PSA ≤ 2 ng/mL: 1/10 (0%) 2 < PSA ≤ 4 ng/mL: 3/9 (33%) 4 < PSA ≤ 10 ng/mL: 4/10 (40%) > 10 ng/mL: 2/8 (25%)
<sup>11</sup> C-choline	Preferential uptake and incorporation into lipid membranes of malignant cells	Localization of recurrent disease in patients with rising PSA after treatment completion	Capable of detecting disease spread to bones, lymph nodes, and distant organs	Disease detection rates too low for initial staging; suboptimal specificity	Detection rates in BCR <sup>25</sup> PSA ≤ 1 ng/mL: 19% 1 < PSA ≤ 2 ng/mL: 25% 2 < PSA ≤ 5 ng/mL: 41% > 5 ng/dL: 67%
<sup>18</sup> F-fluciclovine	Preferential uptake into malignant cells due to upregulated amino acid influx	Localization of recurrent disease in patients with rising PSA after treatment completion	Same as <sup>11</sup> C-choline but with overall better recurrence detection rates	Disease detection rates too low for initial staging; suboptimal specificity	True positive rates in BCR <sup>30</sup> PSA < 1 ng/mL: 21% 1 ≤ PSA < 2 ng/mL: 29% 2 ≤ PSA < 3 ng/mL: 45% ≥ 3 ng/mL: 59%

BCR = biochemical recurrence; PSA = prostate-specific antigen

the notion that this tracer is not useful for imaging this specific malignancy.<sup>4,5</sup> Many prostate cancers are not <sup>18</sup>F-FDG-avid, with one large cohort study reporting a sensitivity of only 37% for the primary tumor.<sup>6</sup> However, <sup>18</sup>F-FDG-PET may still be helpful in specific clinical scenarios, such as for staging high-grade prostate cancers when non-<sup>18</sup>F-FDG tracers are unavailable.<sup>7</sup> In the setting of BCR, <sup>18</sup>F-FDG-PET is likely not informative for most patients. For example, when conventional imaging studies are already negative, <sup>18</sup>F-FDG-PET/

CT localizes the site of recurrence in only 8.1% of cases, Figure 1, according to one study.<sup>8</sup> With respect to metastatic prostate cancer, the number of <sup>18</sup>F-FDG-avid lesions, rather than the degree of <sup>18</sup>F-FDG uptake, has been shown to predict overall survival.<sup>9</sup> Furthermore, as castration-resistant prostate cancer is generally <sup>18</sup>F-FDG-avid, <sup>18</sup>F-FDG-PET can be used to monitor for the development of resistance to androgen deprivation therapy.<sup>7</sup> Similarly, for the neuroendocrine variant of prostate cancer, <sup>18</sup>F-FDG-PET has proven valuable for

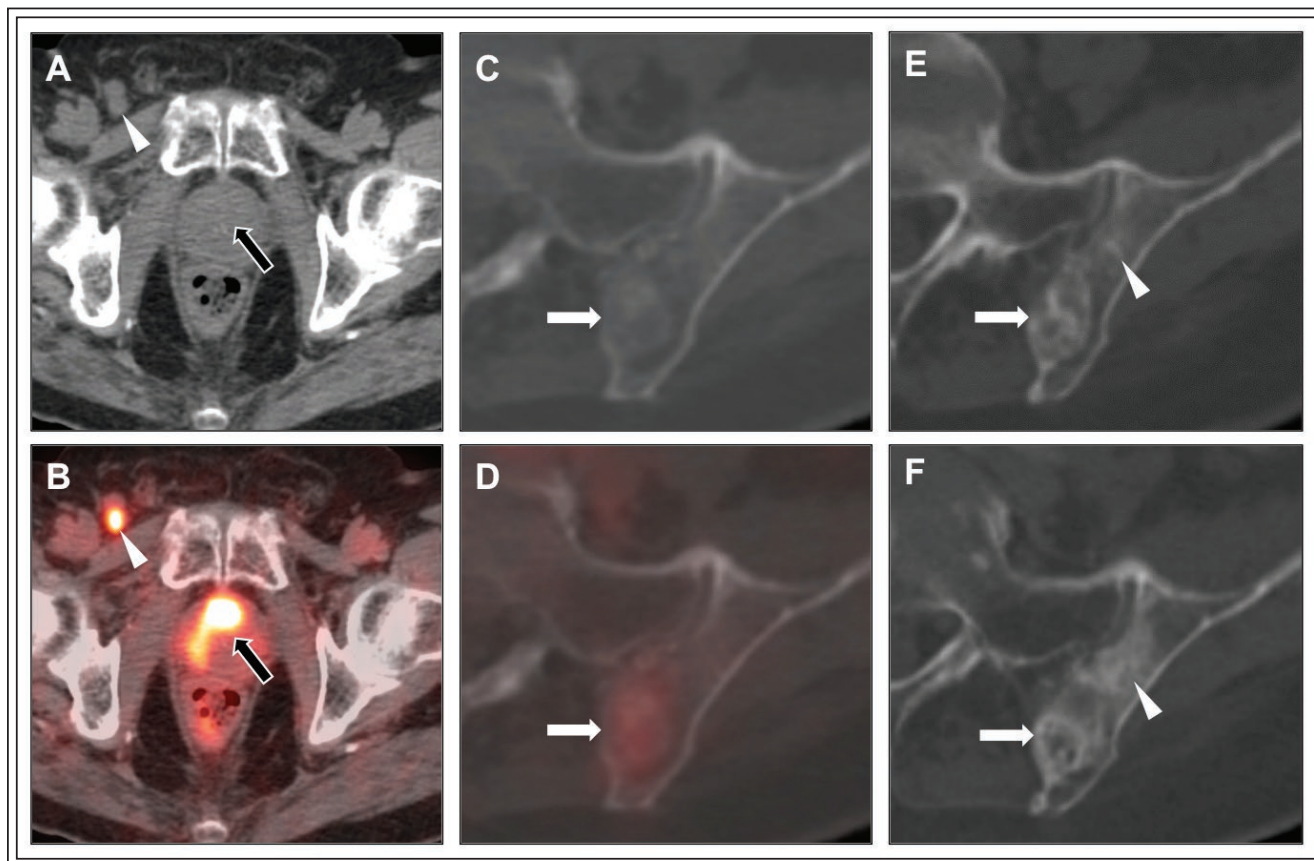


**Figure 1.** Limited utility of <sup>18</sup>F-FDG-PET/CT for prostate cancer. A 71-year-old man with prostate cancer (Gleason 4 + 3) was treated with external beam radiation 10 years prior, followed by several years of androgen deprivation therapy. The patient's PSA subsequently began to rise, so a <sup>18</sup>F-FDG-PET/CT (A-D) was ordered. Note that this study was performed in 2008, before other PET tracers were available at our institution. Transaxial CT images (A, C) with PET fusion (B, D) revealed a markedly FDG-avid lesion centered in the right prostate gland that crossed the midline anteriorly (black arrow in B), though without any correlate on the CT images (black arrow in A). Additionally, there was a normal-sized but FDG-avid (arrowheads in A, B) right inguinal lymph node. These findings were interpreted as consistent with local and nodal disease recurrence. In contrast, a sclerotic lesion in the posterior left iliac bone was only mildly FDG-avid (arrows in C, D) and was deemed indeterminate, despite its suspicious appearance on CT. Subsequent CT scans performed 7 mos (E) and 9 mos (F) later showed continued evolution of this bone lesion (arrows in E, F), as well as development of an additional lesion anteriorly (arrowheads in E, F), corroborating the presence of osseous metastatic disease. This case demonstrates that <sup>18</sup>F-FDG-PET can be limited in the setting of prostate cancer, as lesions can be non-avid or only mildly avid, especially in the context of lower Gleason grade tumors.

the detection of metastatic disease.<sup>10</sup> Overall, <sup>18</sup>F-FDG can occasionally be useful for prostate cancer imaging, though the other PET tracers described below should be preferentially used, if available.

### <sup>18</sup>F-NaF

#### *Background*

Osteoblastic bone lesions are the most common manifestation of metastatic prostate cancer. For many years, osseous staging has relied on <sup>99m</sup>Tc-MDP, a gamma photon emitter that can be imaged using either planar or single photon emission computed tomography

(SPECT) techniques. With the advent of PET, <sup>18</sup>F-NaF (initially described in 1962) has re-emerged as a useful bone imaging agent.<sup>11</sup> The <sup>18</sup>F anions localize to bone by means of exchange with hydroxyl ions on the surface of hydroxyapatite crystals.<sup>12</sup> The main sites of physiologic <sup>18</sup>F-NaF activity are the skeleton, renal collecting system, and urinary bladder. This agent is currently FDA-approved to define areas of altered osteogenic activity, irrespective of etiology.

#### *Evidence supporting clinical use*

There are numerous advantages of <sup>18</sup>F-NaF-PET/CT relative to <sup>99m</sup>Tc-MDP scintigraphy, Figure 2, including

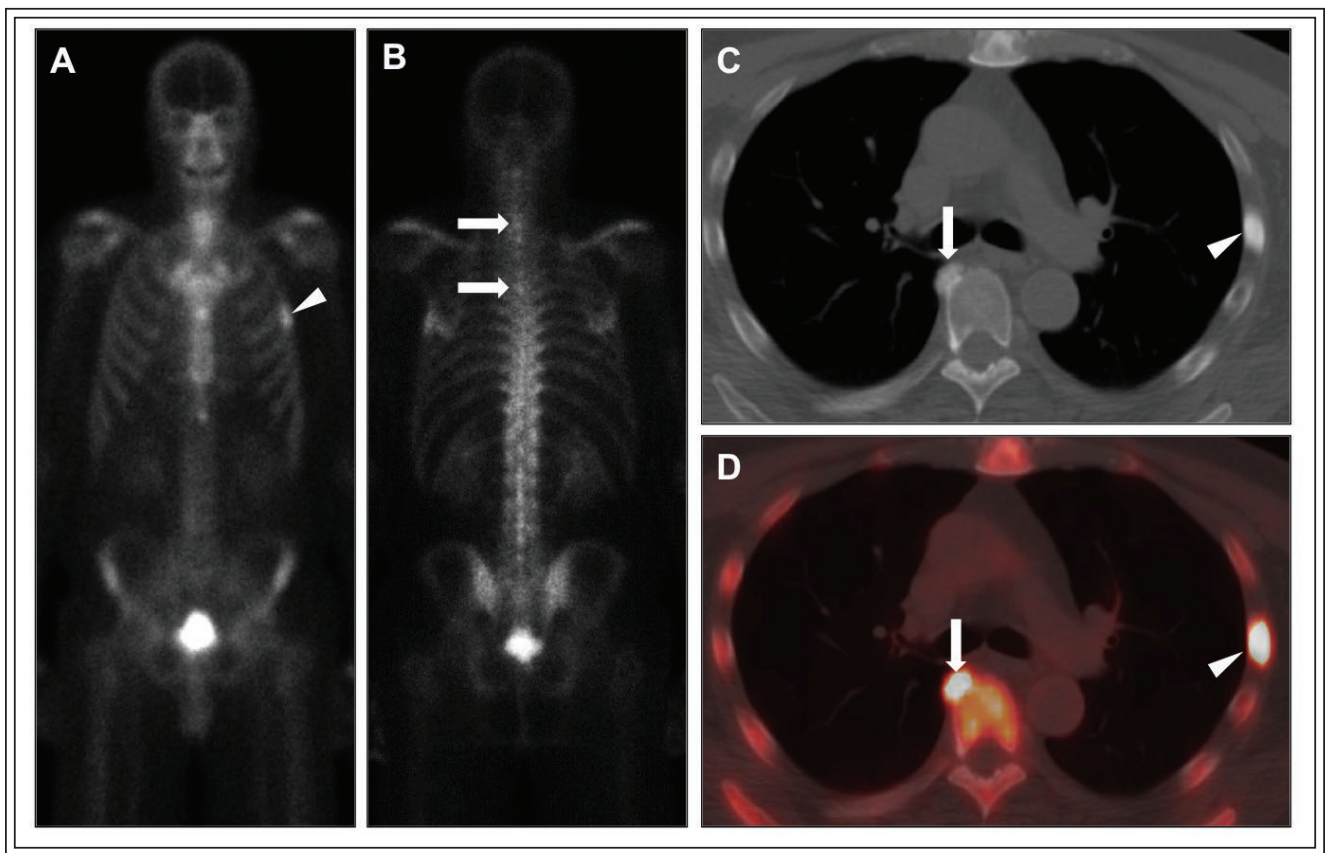


**Figure 2.** Advantages of <sup>18</sup>F-NaF-PET/CT versus <sup>99m</sup>Tc-MDP bone scintigraphy. A 65-year-old man with prostate cancer (Gleason 4 + 5) status-post radical prostatectomy presented for <sup>99m</sup>Tc-MDP bone scintigraphy (A-B) due to a rising PSA. On the anterior view (A), a focus of abnormal uptake identified in the left chest wall (arrowhead) was felt to represent either a metastasis or a rib fracture. On the posterior view (B) several additional foci of mildly increased uptake were seen in the spine (arrows), representing either degenerative change or metastases. The patient subsequently underwent <sup>18</sup>F-NaF-PET/CT (C-D) for further characterization. Transaxial CT images (C) with PET fusion (D) revealed an intense focus of tracer accumulation in the left fourth rib corresponding to a sclerotic osseous lesion (arrowheads) but no evidence of rib fracture. These findings were deemed consistent with a prostate cancer metastasis. In contrast, an additional intense focus of tracer uptake (seen on the initial planar imaging) had the appearance of degenerative change on the CT images (arrows). This case illustrates the advantages of <sup>18</sup>F-NaF-PET/CT over <sup>99m</sup>Tc-MDP bone scans in differentiating malignant from benign etiologies of abnormal osseous metabolism.

higher energy photons, better attenuation correction methods, reduced uptake times, and superior spatial resolution.<sup>13</sup> A study of <sup>18</sup>F-NaF-PET/CT and <sup>99m</sup>Tc-MDP (planar + SPECT) in prostate cancer patients at high risk for bone metastases found overall accuracies of 96% and 80%, respectively.<sup>14</sup> The negative predictive value of <sup>18</sup>F-NaF-PET/CT was 100%, compared with 88.9% for <sup>99m</sup>Tc-MDP. In the setting of PET/MRI, <sup>18</sup>F-NaF-PET may improve the sensitivity of whole-body MRI for osseous metastatic disease.<sup>15</sup> However, a downside of <sup>18</sup>F-NaF-PET is its greater sensitivity for benign processes (e.g., arthritis and fractures), which can make the interpretation of these studies quite time-intensive relative to <sup>99m</sup>Tc-MDP scintigraphy. Importantly, several of the PET tracers discussed in subsequent sections (e.g., <sup>11</sup>C-choline, <sup>68</sup>Ga-PSMA) have also been shown to be more accurate than <sup>99m</sup>Tc-MDP for diagnosing osseous metastases, likely with greater specificity than <sup>18</sup>F-NaF.<sup>16,17</sup> More studies comparing <sup>18</sup>F-NaF to other PET tracers are needed to determine the optimal imaging strategy for diagnosing osseous metastatic disease in both the initial staging and BCR settings.

## <sup>11</sup>C-choline

### *Background*

Choline is a precursor to phosphatidylcholine, a major cell membrane component. Because phosphatidylcholine synthesis is upregulated in malignancy, <sup>11</sup>C-choline was initially devised as a general oncologic PET agent but has mostly gained traction for prostate cancer imaging.<sup>18</sup> Given the short half-life of <sup>11</sup>C (20 min), <sup>18</sup>F-choline (not yet FDA-approved) was developed as an alternative, taking advantage of the relatively long half-life of <sup>18</sup>F (110 min). The main sites of physiologic <sup>11</sup>C-choline uptake are the renal cortex, liver, pancreas, bowel, and salivary glands. Additionally, <sup>18</sup>F-choline accumulates in the collecting systems and urinary bladder.<sup>19</sup> At present, <sup>11</sup>C-choline is FDA-approved for identifying sites of disease in patients with BCR.

### *Evidence supporting clinical use*

Among patients with newly diagnosed intermediate/high risk prostate cancer, <sup>11</sup>C-choline has sensitivities for nodal metastatic disease of 60% and 41% on a per-patient basis and a per-node basis, respectively.<sup>20</sup> Furthermore, <sup>11</sup>C-choline performs relatively poorly for assessing the presence and/or extent of intraprostatic tumors, with false positives attributable to conditions such as benign prostatic hyperplasia (BPH).<sup>21</sup> Although its detection accuracy is prohibitively low for initial staging, <sup>11</sup>C-choline has proven more valuable for re-staging indications.<sup>22</sup>

A recent meta-analysis found <sup>11</sup>C-choline-PET/CT to have a pooled detection rate of 62% for recurrent disease at any location.<sup>23</sup> Importantly, localizing disease recurrence to a particular site can significantly impact management, ranging from salvage radiation for recurrence in the prostatectomy bed to systemic hormonal therapy for distant metastases.<sup>24</sup> Studies have also found that higher PSA levels and shorter PSA doubling times predict greater detection rates of <sup>11</sup>C-choline-PET/CT for disease recurrence, suggesting that PSA-based metrics could be used to improve the utility of <sup>11</sup>C-choline-PET/CT for patients with BCR.<sup>25</sup>

In the realm of PET/MRI, simultaneous <sup>18</sup>F-choline-PET/ multiparametric MRI (mpMRI) outperforms mpMRI alone with respect to sensitivity and accuracy for the initial diagnosis of prostate cancer.<sup>26</sup> Interestingly, quantitative biomarkers derived from a simultaneous <sup>18</sup>F-choline-PET/MRI (e.g., MRI-assisted metabolic tumor volume) performed 1 week prior to radical prostatectomy are better predictors of pathologic findings (e.g., perineural invasion, lymphatic invasion, extracapsular extension) than more conventional PET or MRI parameters.<sup>27</sup> Although <sup>11</sup>C-choline-PET may be of relatively minimal value for initial staging, it can play an important role in localizing disease recurrence and optimizing subsequent treatment strategies, Figure 3.

## <sup>18</sup>F-fluciclovine

### *Background*

Similar to choline, various amino acids undergo increased uptake by malignant cells.<sup>28</sup> Taking advantage of this phenomenon, <sup>18</sup>F-fluciclovine (also known as Axumin or <sup>18</sup>F-FACBC) is a radiolabeled synthetic amino acid that has been investigated as a PET tracer for prostate cancer. The main sites of physiologic <sup>18</sup>F-fluciclovine uptake are the pancreas, liver, bone marrow, and salivary glands, with relatively little urinary excretion.<sup>19</sup> As with <sup>11</sup>C-choline, <sup>18</sup>F-fluciclovine is currently FDA-approved for localizing disease sites in BCR.

### *Evidence supporting clinical use*

In one study of patients with BCR and no evidence of metastatic disease on <sup>99m</sup>Tc-MDP bone scans, <sup>18</sup>F-fluciclovine-PET/CT had a sensitivity of 90.2% and detected significantly more prostatic and extraprostatic recurrences than the gamma photon emitter <sup>111</sup>In-capromab pentetide (ProstaScint).<sup>29</sup> Similarly, a head-to-head comparison of <sup>18</sup>F-fluciclovine with <sup>11</sup>C-choline in patients with BCR after prostatectomy found significantly higher detection rates for <sup>18</sup>F-fluciclovine at low, intermediate, and high PSA levels.<sup>30</sup> With respect to initial staging, <sup>18</sup>F-fluciclovine demonstrates

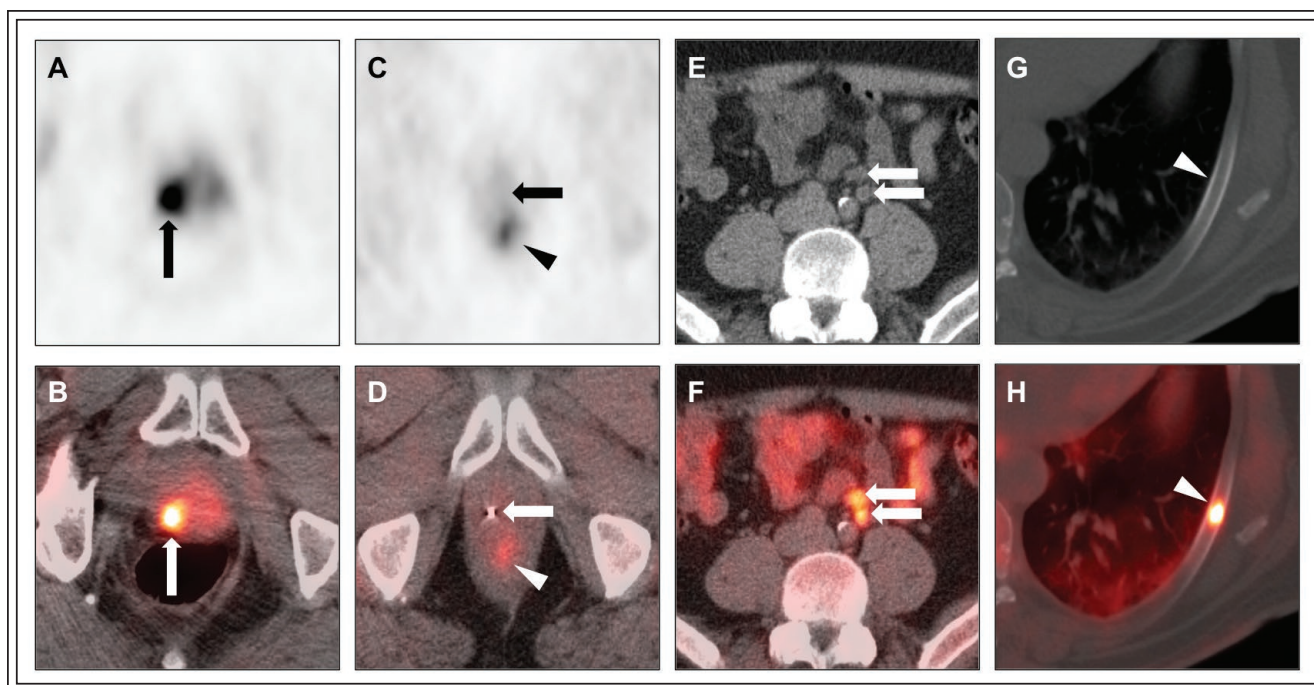


**Figure 3.** Value of  $^{11}\text{C}$ -choline-PET/CT for localizing disease recurrence. **(A-B)** A 73-year-old man with prostate cancer (Gleason 3 + 3) status-post external beam radiation therapy 10 years prior presented for a  $^{11}\text{C}$ -choline-PET/CT due to a rising PSA. Transaxial PET images **(A)** with CT fusion **(B)** revealed a focus of marked uptake centered in the right peripheral zone of the prostate, consistent with locally recurrent disease. There were no other sites of abnormal tracer uptake to suggest nodal or distant metastatic disease. **(C-H)** A 62-year-old man with prostate cancer (Gleason 3 + 4) status-post radical prostatectomy 9 years prior, followed by salvage radiation to the surgical bed 7 years prior for a rising PSA, presented for a  $^{11}\text{C}$ -choline-PET/CT due to BCR. Transaxial PET images **(C)** with CT fusion **(D)** showed no suspicious activity in the surgical bed (arrow in **C**). A fiducial marker was visible (arrow in **D**). Note mild physiologic tracer uptake in the rectum (arrowheads). However, transaxial CT images **(E, G)** with PET fusion **(F, H)** also revealed several tracer-avid normal-sized left retroperitoneal nodes (arrows in **E, F**) and a focus of abnormal uptake in the left seventh rib without a correlate on the CT images (arrowheads in **G, H**). These findings were interpreted as consistent with metastatic disease, as confirmed on subsequent biopsy of the left rib lesion. These two cases demonstrate the ability of  $^{11}\text{C}$ -choline-PET to identify sites of BCR in locations where the disease might not be apparent on the CT images alone.

greater uptake in prostate cancers than in normal prostatic tissue but localizes to prostate cancers and BPH nodules with similar avidity.<sup>31</sup> Another study of 68 patients comparing  $^{18}\text{F}$ -fluciclovine-PET/CT to conventional imaging (i.e., CT,  $^{99\text{m}}\text{Tc}$ -MDP bone scans) found similar overall accuracies (85.5% vs. 87.3%, respectively) for initial staging but noted that  $^{18}\text{F}$ -fluciclovine-PET/CT detected sites of nodal (13 patients; 19%) and skeletal (7 patients; 10%) disease missed by conventional imaging.<sup>32</sup> Thus, although its proper role in initial staging has not yet been established,  $^{18}\text{F}$ -fluciclovine-PET is valuable for localizing recurrent prostate cancer, Figure 4, and has demonstrated superior performance relative to  $^{11}\text{C}$ -choline-PET for this indication, as described above.

## PSMA tracers

Targeting mechanisms, imaging indications, and relative strengths/weaknesses of the PSMA tracers, as well as relevant PSA values, are summarized in Table 2.

### Background

PSMA is a transmembrane protein that is expressed at low levels in normal prostatic parenchyma and BPH but upregulated in prostate cancer, as well as several other malignancies.<sup>33</sup> Like  $^{111}\text{In}$ -capromab pentetide (ProstaScint), the initial PET tracers targeting PSMA were monoclonal antibodies. In contrast, the more recent cohort of PSMA tracers consists of radiolabeled urea-based small molecule ligands, most notably  $^{68}\text{Ga}$ -PSMA-

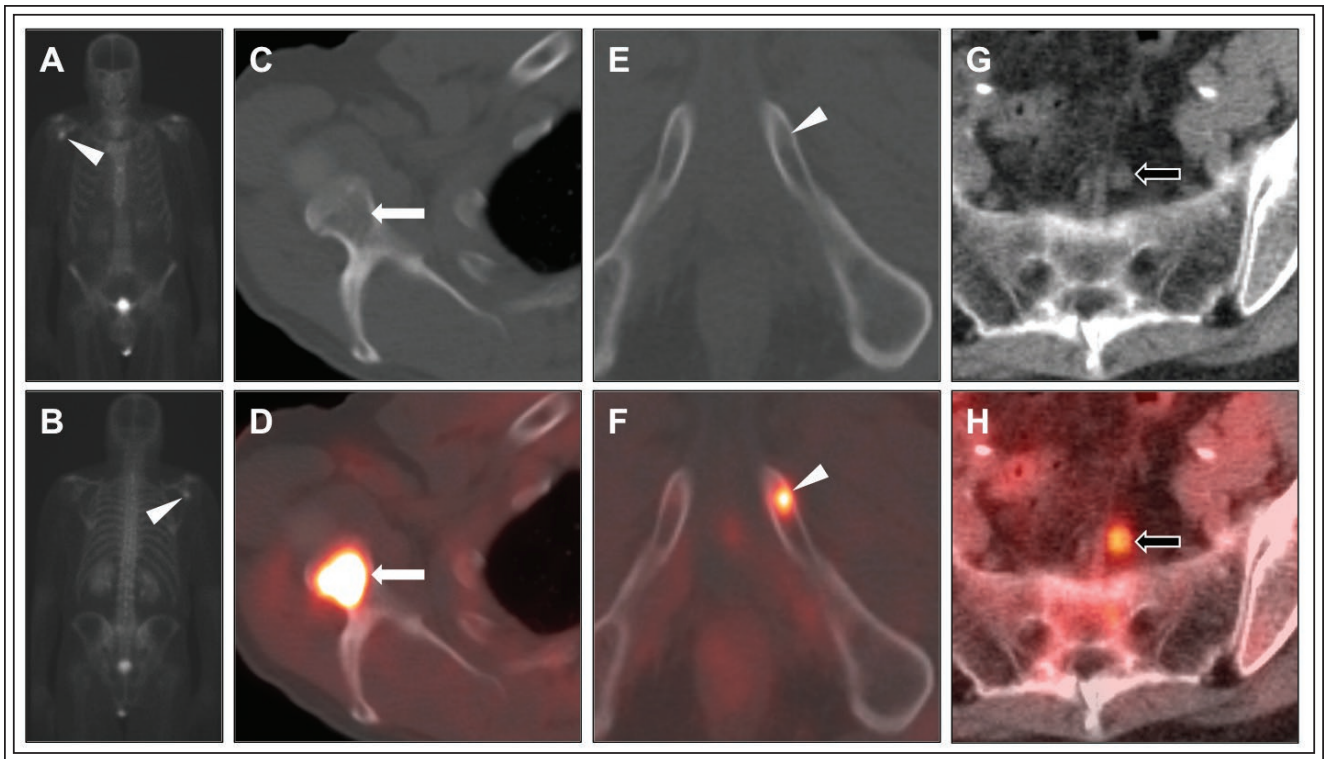


**Figure 4.** Value of  $^{18}\text{F}$ -fluciclovine-PET/CT for localizing disease recurrence. A 67-year-old man with prostate cancer (Gleason 4 + 5) status-post radical prostatectomy 1 year prior underwent a  $^{99\text{m}}\text{Tc}$ -MDP bone scan (**A**, **B**) due to a rising PSA. Anterior (**A**) and posterior (**B**) views revealed a solitary focus of increased tracer uptake in the right glenoid region (arrowheads) that was interpreted as metastatic disease versus degenerative change. A  $^{18}\text{F}$ -fluciclovine-PET/CT (**C**-**H**) was ordered for further evaluation. Transaxial CT images (**C**, **E**, **G**) with PET fusion (**D**, **F**, **H**) showed a markedly tracer-avid lesion in the right glenoid (white arrow in **D**), without a definite correlate on the CT images (white arrow in **C**). Similarly, there was an additional tracer-avid lesion in the left inferior pubic ramus (arrowhead in **F**), without a definite correlate on the CT images (arrowhead in **E**). Even in retrospect, this pelvic lesion was not appreciable on the  $^{99\text{m}}\text{Tc}$ -MDP bone scan. Furthermore, a relatively inconspicuous subcentimeter presacral lymph node (black arrow in **G**) was also tracer-avid (black arrow in **H**). Percutaneous biopsy of the right glenoid lesion confirmed metastatic prostate cancer. This case shows the potential of  $^{18}\text{F}$ -fluciclovine to identify sites of BCR that are not detectable by either conventional bone scintigraphy or CT.

HBED-CC ( $^{68}\text{Ga}$ -PSMA) and  $^{18}\text{F}$ -DCFPyL ( $^{18}\text{F}$ -PyL), though neither agent is currently FDA-approved.<sup>34</sup> These agents bind to the extracellular component of PSMA, unlike  $^{111}\text{In}$ -capromab pendetide, which binds only to the intracellular component (thereby limiting sensitivity). Sites of potential physiologic uptake of these PSMA ligands include the kidneys, collecting systems and urinary bladder, salivary/lacrimal glands, spleen, liver, and intestines.<sup>35</sup>

#### *Evidence supporting clinical use*

In the setting of BCR, the utility of PSMA-PET for localizing anatomic sites of recurrence, Figure 5, increases in tandem with PSA levels, with detection rates ranging from 42% at PSAs < 0.2 ng/mL to 95% at PSAs > 2 ng/mL.<sup>36</sup>

Importantly, PSMA-PET has been shown to outperform the non-PSMA PET tracers for disease localization in BCR, particularly at low PSA levels (e.g., 50% for  $^{68}\text{Ga}$ -PSMA-PET/CT versus 12.5% for  $^{18}\text{F}$ -choline-PET/CT at PSAs < 0.5 ng/mL).<sup>37</sup> Furthermore,  $^{68}\text{Ga}$ -PSMA-PET/mpMRI has proven superior to  $^{68}\text{Ga}$ -PSMA-PET/CT for the detection of local recurrence in the prostatectomy bed.<sup>38</sup>

$^{68}\text{Ga}$ -PSMA-PET is also valuable in the setting of initial staging. For example, a study of 130 patients with intermediate/high risk prostate cancer found that  $^{68}\text{Ga}$ -PSMA-PET outperforms conventional imaging (CT or MRI) for assessing nodal involvement, using histology from pelvic lymph node dissection as the standard of reference.<sup>39</sup> On a per-patient basis, the sensitivities, specificities, and overall accuracies were 65.9%, 98.9%,

TABLE 2. PSMA-targeted PET tracers

PET tracer	Mechanism of targeting	Imaging indications	Strengths	Weaknesses	Relevant PSA ranges
<sup>68</sup> Ga-PSMA-HBED-CC	Binding to PSMA, which is over-expressed by prostate cancer cells	Potential roles in initial staging, suspected recurrence, treatment response assessment	More specificity for prostate cancer than <sup>11</sup> C-choline or <sup>18</sup> F-fluciclovine	Not yet FDA-approved	Detection rates in BCR <sup>36</sup> PSA < 0.2 ng/mL: 42% 0.2 ≤ PSA < 1 ng/mL: 58% 1 ≤ PSA < 2 ng/mL: 76% ≥ 2 ng/mL: 95%
<sup>18</sup> F-DCFPyL	Binding to PSMA, which is over-expressed by prostate cancer cells	Potential roles in initial staging, suspected recurrence, treatment response assessment	Same as <sup>68</sup> Ga-PSMA-HBED-CC but with longer half-life and better spatial resolution	Not yet FDA-approved	Detection rates in BCR Not well-defined but likely as good or better than those cited above for <sup>68</sup> Ga-PSMA-HBED-CC

BCR = biochemical recurrence; PSA = prostate-specific antigen

and 88.5% for <sup>68</sup>Ga-PSMA-PET versus 43.9%, 85.4%, and 72.3% for conventional imaging alone. <sup>68</sup>Ga-PSMA-PET is also capable of delineating primary cancers within the prostate itself, Figure 6, and the degree of PSMA expression (which in turn determines the

level of tracer uptake) appears to correlate with tumor aggressiveness.<sup>33</sup> As such, an objective assessment of tracer uptake by primary prostate cancers has been incorporated into the recently proposed molecular imaging TNM (miTNM) system, which includes an

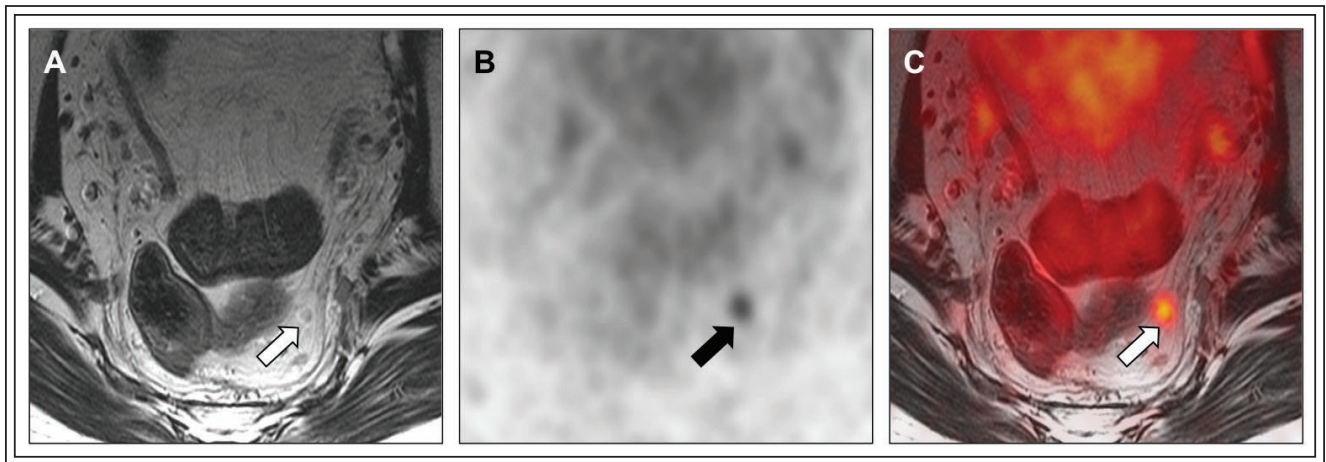


**Figure 5.** Value of <sup>68</sup>Ga-PSMA-PET/MRI for localizing disease recurrence. A 59-year-old man with prior prostate cancer status-post radical prostatectomy with subsequent BCR (PSA = 0.41 ng/mL) underwent <sup>68</sup>Ga-PSMA-PET/MRI. On the transaxial T2-weighted MR images (A), there were no grossly enlarged lymph nodes and no abnormal soft tissue in the prostatectomy bed (not shown). A normal-appearing left mesorectal lymph node on the MR images (arrow in A) corresponded to a focus of tracer uptake on the transaxial PET images (arrow in B), as shown to great advantage on the fused PET/MRI images (arrow in C), consistent with a site of recurrent disease. This case shows the value of PSMA-PET for disease localization in the setting of BCR, though it should be noted that the ability of this imaging modality to detect recurrent disease is greater at higher PSA levels.

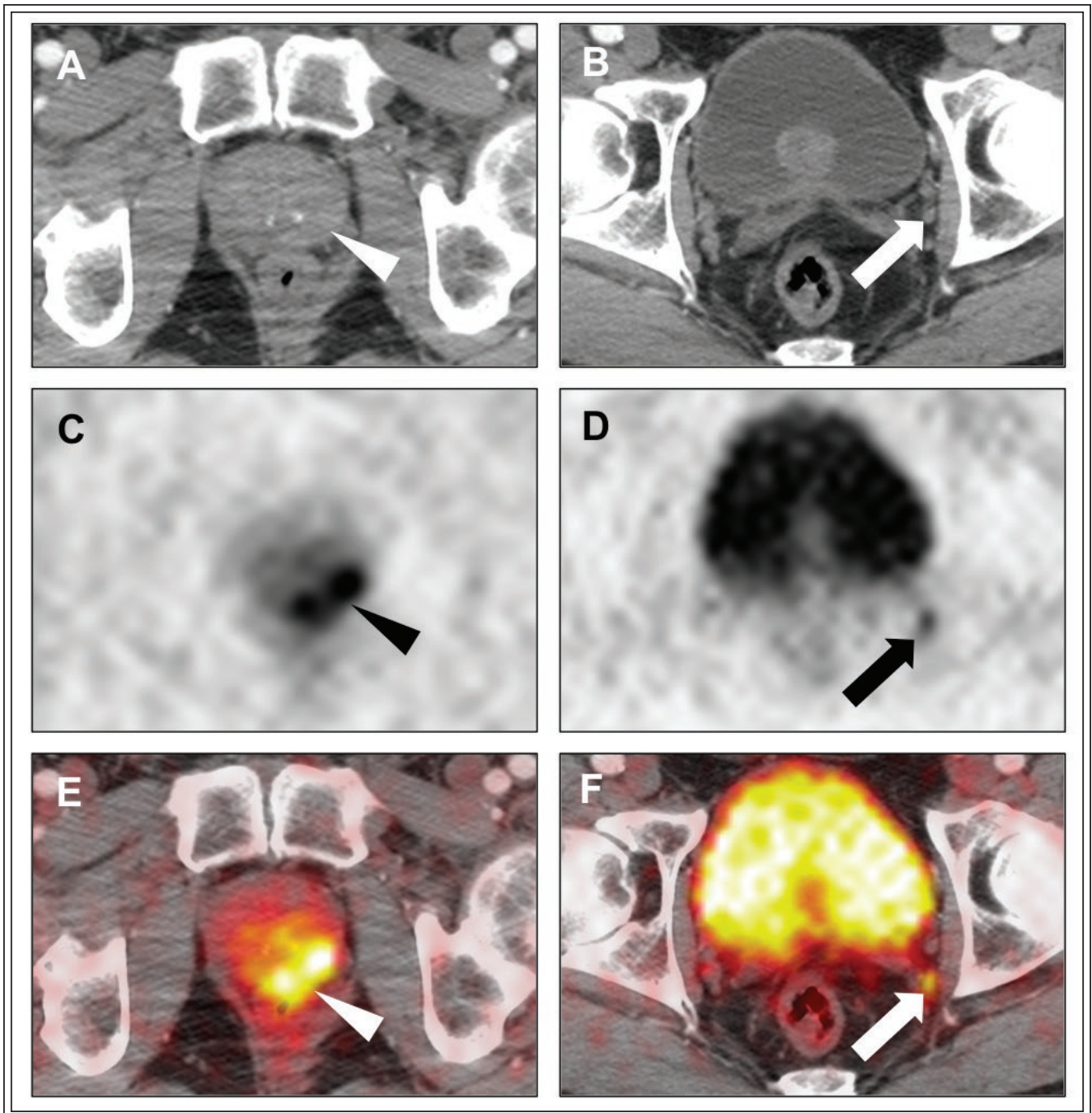


**Figure 6.** Ability of  $^{68}\text{Ga}$ -PSMA-PET/CT to identify the primary tumor site. A 67-year-old man with Gleason 4 + 3 prostate cancer in the left prostate gland on transrectal ultrasound-guided biopsy underwent  $^{68}\text{Ga}$ -PSMA-PET/CT for initial staging. Transaxial CT (A-B),  $^{68}\text{Ga}$ -PSMA-PET (C-D), and fused  $^{68}\text{Ga}$ -PSMA-PET/CT (E-F) images at the level of the prostate gland (A, C, E) and more superiorly at the level of the bladder (B, D, F) are shown. A focus of intense tracer uptake in the left peripheral zone of the prostate without a definite CT correlate (arrowheads) corresponded to the site of disease on the prior biopsy. A small left obturator lymph node without suspicious morphologic features (arrow in B) also exhibited increased tracer uptake (arrows in D, F), suspicious for a nodal metastasis. Subsequent radical prostatectomy with pelvic lymph node dissection (PLND) confirmed the presence of Gleason 5 + 4 disease in the left obturator node. This case demonstrates the strengths of PSMA-PET with respect to delineating high-grade cancers within the prostate gland itself and detecting nodal metastatic disease.

interpretation schema for initial staging examinations with PSMA-PET.<sup>40</sup> Finally, simultaneous <sup>68</sup>Ga-PSMA-PET/mpMRI has been shown to improve both pre-prostatectomy tumor localization and diagnostic accuracy compared with either modality alone.<sup>41</sup>

Overall, the PSMA ligands represent promising PET tracers and warrant further investigation to define their optimal clinical roles in the North American practice setting, though these tracers are already in widespread clinical use throughout Europe.

## Other emerging tracers

According to the United States National Institutes of Health's ClinicalTrials.gov website, there are currently about 60-70 registered studies pertaining to the use of PET tracers in prostate cancer that are listed as active and/or recruiting.<sup>42</sup> These investigational PET tracers are summarized in Table 3 and described in greater detail below by tracer class.

### Other PSMA tracers

The majority of active clinical trials are focused on the small molecule PSMA tracers <sup>68</sup>Ga-PSMA and <sup>18</sup>F-PyL. Although these agents have already proven to be valuable

for targeting PSMA expression (as discussed above), more recent work has focused on the humanized monoclonal anti-PSMA antibody J591 and its derivative antibody fragment IAB2M. Full antibody agents, such as <sup>89</sup>Zr-J591, typically do not achieve ideal tumor-to-background ratios until nearly a week after administration due to their slow clearance from the blood pool.<sup>43</sup> In contrast, <sup>89</sup>Zr-IAB2M, as an antibody fragment, can be effectively imaged at 48 hours.<sup>44</sup> As a consequence, <sup>89</sup>Zr-J591 is no longer under development. Compared with the small molecule PSMA-targeting agents, the antibody agents offer some unique advantages. For example, due to its large size, <sup>89</sup>Zr-IAB2M does not undergo renal clearance, thus reducing background urinary activity and enhancing lesion detection. Furthermore, there have been several studies utilizing the long bioavailability of antibody-based anti-PSMA agents to deliver therapeutic radiation doses to prostate cancer cells (e.g., via coupling to <sup>177</sup>Lu).<sup>42</sup>

### AR tracers

The androgen receptor (AR) is expressed by benign prostate tissue, as androgens are essential to normal prostatic growth and functioning. However, the AR is also expressed in prostate cancer, and the activation of this receptor is a key driver of prostate cancer growth.

TABLE 3. Emerging PET tracers for prostate cancer

Tracer class	Tracer mechanism	Example tracers
PSMA <sup>43,44</sup>	Binding to PSMA, which is over-expressed by prostate cancer cells	<sup>89</sup> Zr-IAB2M
Androgen receptor <sup>45,46</sup>	Preferential uptake by prostate cancer cells due to androgen receptor over-expression	<sup>18</sup> F-FDHT, <sup>18</sup> F-FMDHT
Amino acid transport <sup>47,48</sup>	Preferential uptake into malignant cells due to upregulated amino acid influx	<sup>11</sup> C-methionine, <sup>11</sup> C-sarcosine
Lipid metabolism <sup>49,50</sup>	Preferential uptake into malignant cells due to upregulated membrane synthesis and turnover	<sup>11</sup> C-acetate, <sup>18</sup> F-fluorocholine, <sup>18</sup> F-fluoroethylcholine
GRPR (bombesin receptor) <sup>52</sup>	Direct antagonistic binding to GRPR, which is over-expressed by prostate cancer cells	<sup>68</sup> Ga-RM2, <sup>68</sup> Ga-MJ9
Hypoxia <sup>53,54</sup>	Preferential uptake at sites of low oxygen concentration, such as in aggressive tumors	<sup>18</sup> F-FMISO, <sup>18</sup> F-FAZA
DNA synthesis <sup>55-57</sup>	Preferential uptake into cancer cells due to upregulated DNA synthesis for rapid cell division	<sup>18</sup> F-FMAU, <sup>18</sup> F-FLT
Other <sup>58-60</sup>	Targeting of uPAR, VPAC1, STEAP1, etc.	<sup>68</sup> Ga-AE105, <sup>64</sup> Cu-TP3805, <sup>89</sup> Zr-MSTP2109A

PSMA = prostate-specific membrane antigen; FDHT = 16-beta-fluoro-5-alpha-dihydrotestosterone; GRPR = gastrin-releasing peptide receptor; FMISO = fluoromisonidazole; FAZA = fluoroazomycin arabinoside; uPAR = urokinase-type plasminogen activator receptor; VPAC1 = vasoactive intestinal polypeptide receptor 1; STEAP1 = six-transmembrane epithelial antigen of prostate member 1

Accordingly, many therapies for high risk and metastatic prostate cancer involve androgen deprivation therapy to reduce activation of the AR (e.g., gonadotropin-releasing hormone [GnRH] agonists, direct AR inhibitors). Furthermore, the AR and its downstream signaling pathways play an important role in the development of castration resistance.<sup>45</sup> Specifically, in the setting of androgen deprivation therapy, the development of castration resistance is associated with mutations that permit ligand-independent activation of the AR or AR-independent activation of the downstream pathways. Accordingly, imaging with radiolabeled androgen analogs, such as <sup>18</sup>F-fluoro-5 $\alpha$ -dihydrotestosterone (<sup>18</sup>F-FDHT), offers a means of interrogating the AR pathway in patients with apparent castration-resistant prostate cancer.<sup>46</sup> AR imaging may also be valuable in assessing for adequate pharmacologic AR blockade in patients receiving anti-androgen therapies.

#### *Amino acid transport tracers*

Similar to <sup>18</sup>F-FACBC, which takes advantage of the increased protein synthesis requirements of prostate cancer cells, a variety of additional radiolabeled amino acid derivatives have been under evaluation for use in prostate cancer imaging.<sup>47</sup> These agents include <sup>11</sup>C-methionine, <sup>11</sup>C-sarcosine, and <sup>11</sup>C-methylaminoisobutyric acid (MeAIB). For instance, <sup>11</sup>C-sarcosine was recently shown to have a higher tumor-to-background ratio than <sup>11</sup>C-choline in a preclinical model of prostate cancer.<sup>48</sup> However, in recent years, interest in the <sup>11</sup>C-labeled amino acid derivatives has decreased due to (1) the short half-life of <sup>11</sup>C (20 minutes), which makes imaging less convenient due to the resultant shorter useful imaging window, and (2) the FDA-approval of <sup>18</sup>F-FACBC. Accordingly, there are few active clinical trials utilizing these agents.<sup>42</sup>

#### *Lipid metabolism tracers*

Acetate, like choline, is an important substrate of membrane lipid syntheses, a process that is highly upregulated in malignant cells due to their rapid growth.<sup>49</sup> Although <sup>11</sup>C-acetate initially gained traction in the imaging of myocardial metabolism, it has been investigated in the initial staging of prostate cancer and in localizing sites of BCR.<sup>49</sup> For example, a study of 23 patients with rising PSA after prostatectomy demonstrated similar diagnostic performance for <sup>11</sup>C-acetate and <sup>18</sup>F-fluorocholine in identifying sites of disease recurrence, with <sup>11</sup>C-acetate having the added advantage of low urinary excretion due to respiratory clearance in the form of <sup>11</sup>C-CO<sub>2</sub>.<sup>50</sup> The role of <sup>11</sup>C-acetate in prostate cancer remains unclear, but it may prove useful in confirming inhibition of fatty acid synthesis by chemotherapeutics targeting this pathway.<sup>51</sup>

#### *GRPR tracers*

The gastrin-releasing peptide receptor (GRPR), a member of the bombesin receptor family, is upregulated in a variety of cancers, including prostate cancer.<sup>52</sup> The main sites of physiologic uptake of the GRPR tracers include the pancreas, kidneys, bladder, liver, spleen, and gastrointestinal tract. <sup>68</sup>Ga-based and <sup>18</sup>F-based GRPR tracers have demonstrated initial success in the identification of sites of biochemically recurrent prostate cancer. Tracers within this family currently under investigation for the detection of primary and/or recurrent prostate cancer include <sup>68</sup>Ga-RM2, <sup>68</sup>Ga-MJ9, and <sup>18</sup>F-MATBBN.<sup>42</sup>

#### *Hypoxia tracers*

Hypoxia is a state of reduced oxygen tension that is characteristically present in the microenvironments of aggressive solid tumors.<sup>53</sup> Prostate cancer has a highly variable clinical course, and hypoxia imaging may represent an approach for risk stratification of prostate cancer due to the association between tumor hypoxia and metastatic disease, recurrence after treatment, and overall poor outcomes. There are multiple hypoxia-based PET imaging agents, such as <sup>18</sup>F-FMISO, <sup>18</sup>F-HX4, and <sup>18</sup>F-FAZA,<sup>54</sup> that are currently under evaluation in prostate cancer.<sup>42</sup> However, evidence to date has not substantiated the presence of clinically significant hypoxia in primary prostate cancers.<sup>53</sup> Thus, the role of hypoxia imaging remains undefined.

#### *DNA synthesis tracers*

Radiolabeled derivatives of DNA are taken up preferentially by malignant cells due to upregulation of DNA synthesis in the setting of increased cellular proliferation.<sup>55</sup> The tracers <sup>18</sup>F-FMAU and <sup>18</sup>F-FLT, which are analogues of DNA precursors, have demonstrated preclinical and early clinical feasibility in prostate cancer.<sup>56,57</sup> These agents have high uptake in the liver and renal cortex; moderate uptake in the spleen, heart, and salivary glands; and relatively low uptake in bone marrow. Studies using these agents in other solid tumors have demonstrated rapid declines in radiotracer uptake after the initiation of therapy, suggesting a role in the early assessment of treatment response.<sup>55</sup>

#### *Additional tracers*

Various additional PET radiotracers may play a future role in prostate cancer imaging. For instance, <sup>64</sup>Cu-TP3805 has a strong affinity for the VPAC1 receptor, a G-protein coupled receptor that is overexpressed in prostate cancer but minimally expressed on benign prostate tissue.<sup>58</sup> The cell surface protein 6 transmembrane epithelial antigen of prostate 1 (STEAP1)

has also been identified as a target in castration-resistant prostate cancer. The monoclonal antibody MSTP2109A, which binds to STEAP1, has been developed as an experimental therapeutic agent, and the corresponding PET radiotracer  $^{89}\text{Zr}$ -MSTP2109A has been tested as an imaging agent for castration-resistant prostate cancer.<sup>59</sup> Finally,  $^{68}\text{Ga}$ -AE105 has been developed for imaging of the urokinase-type plasminogen activator receptor (uPAR), which is overexpressed by many cancers.<sup>60</sup> In the setting of prostate cancer, the degree of uPAR expression is proportional to tumor aggressiveness. Although these new tracers are promising, much work is still needed to establish their role in clinical practice.

## Conclusions

Although  $^{18}\text{F}$ -FDG-PET may be useful in certain clinical scenarios, there are many new PET tracers targeting other aspects of prostate cancer biology that have already proven more valuable for both initial staging and detecting recurrent disease. Specifically,  $^{18}\text{F}$ -NaF is capable of diagnosing osseous metastases with a higher degree of sensitivity and specificity than conventional bone scans, whereas  $^{11}\text{C}$ -choline and  $^{18}\text{F}$ -fluciclovine can often identify sites of BCR better than standard anatomic imaging modalities such as CT or MRI. The optimal role of the PSMA tracers has not yet been defined but may include preoperative nodal staging and/or localizing recurrent disease. Furthermore, there are many new promising classes of prostate cancer PET tracers on the horizon. □

---

## References

- Heiden MG Vander, Cantley LC, Thompson CB. Understanding the warburg effect: the metabolic requirements of cell proliferation. *Science* 2009;324(5930):1029-1033.
- Cohade C. Altered biodistribution on FDG-PET with emphasis on brown fat and insulin effect. *Semin Nucl Med* 2010;40(4):283-293.
- CMS. Decision memo for positron emission tomography (FDG) for solid tumors (CAG-00181R4). Available at: <https://www.cms.gov/medicare-coverage-database/details/nca-decision-memo.aspx?NCAId=263>. Accessed February 25, 2018.
- Salminen E, Hogg A, Binns D, Frydenberg M, Hicks R. Investigations with FDG-PET scanning in prostate cancer show limited value for clinical practice. *Acta Oncol* 2002;41(5):425-429.
- Hofer C, Laubenbacher C, Block T, Breul J, Hartung R, Schwaiger M. Fluorine-18-fluorodeoxyglucose positron emission tomography is useless for the detection of local recurrence after radical prostatectomy. *Eur Urol* 1999;36(1):31-35.
- Minamimoto R, Senda M, Jinnouchi S et al. The current status of an FDG-PET cancer screening program in Japan, based on a 4-year (2006-2009) nationwide survey. *Ann Nucl Med* 2013;27(1):46-57.
- Jadvar H. Is there use for FDG-PET in prostate cancer? *Semin Nucl Med* 2016;46(6):502-506.
- Jadvar H, Desai B, Ji L et al. Prospective evaluation of  $^{18}\text{F}$ -NaF and  $^{18}\text{F}$ -FDG PET/CT in detection of occult metastatic disease in biochemical recurrence of prostate cancer. *Clin Nucl Med* 2012;37(7):637-643.
- Vargas HA, Wassberg C, Fox JJ et al. Bone metastases in castration-resistant prostate cancer: associations between morphologic CT patterns, glycolytic activity, and androgen receptor expression on PET and overall survival. *Radiology* 2014;271(1):220-229.
- Spratt DE, Gavane S, Tarlinton L et al. Utility of FDG-PET in clinical neuroendocrine prostate cancer. *Prostate* 2014;74(11):1153-1159.
- Bastawrous S, Bhargava P, Behnia F, Djang DSW, Haseley DR. Newer PET application with an old tracer: role of  $^{18}\text{F}$ -NaF skeletal PET/CT in oncologic practice. *Radiographics* 2014;34(5):1295-1316.
- Weber DA, Greenberg EJ, Dimich A et al. Kinetics of radionuclides used for bone studies. *J Nucl Med* 1968;10(1):8-17.
- Kulshrestha RK, Vinjamuri S, England A, Nightingale J, Hogg P. The role of  $^{18}\text{F}$ -sodium fluoride PET/CT bone scans in the diagnosis of metastatic bone disease from breast and prostate cancer. *J Nucl Med Technol* 2016;44(4):217-222.
- Withofs N, Grayet B, Tancredi T et al.  $^{18}\text{F}$ -fluoride PET/CT for assessing bone involvement in prostate and breast cancers. *Nucl Med Commun* 2011;32(3):168-176.
- Minamimoto R, Loening A, Jamali M et al. Prospective comparison of  $^{99\text{m}}\text{Tc}$ -MDP scintigraphy, combined  $^{18}\text{F}$ -NaF and  $^{18}\text{F}$ -FDG PET/CT, and whole-body MRI in patients with breast and prostate cancer. *J Nucl Med* 2015;56(12):1862-1868.
- Janssen J-C, Meißner S, Woythal N et al. Comparison of hybrid  $^{68}\text{Ga}$ -PSMA-PET/CT and  $^{99\text{m}}\text{Tc}$ -DPD-SPECT/CT for the detection of bone metastases in prostate cancer patients: Additional value of morphologic information from low dose CT. *Eur Radiol* 2017;28(2):610-619.
- Kitajima K, Fukushima K, Yamamoto S et al. Diagnostic performance of  $^{11}\text{C}$ -choline PET/CT and bone scintigraphy in the detection of bone metastases in patients with prostate cancer. *Nagoya J Med Sci* 2017;79(3):387-399.
- Cuccurullo V, Di Stasio GD, Evangelista L, Castoria G, Mansi L. Biochemical and pathophysiological premises to positron emission tomography with choline radiotracers. *J Cell Physiol* 2017;232(2):270-275.
- Schuster DM, Nanni C, Fanti S. PET tracers beyond FDG in prostate cancer. *Semin Nucl Med* 2016;46(6):507-521.
- Schiavina R, Scattoni V, Castellucci P et al.  $^{11}\text{C}$ -choline positron emission tomography/computerized tomography for preoperative lymph-node staging in intermediate-risk and high-risk prostate cancer: comparison with clinical staging nomograms. *Eur Urol* 2008;54(2):392-401.
- Farsad M, Schiavina R, Castellucci P et al. Detection and localization of prostate cancer: correlation of  $^{11}\text{C}$ -choline PET/CT with histopathologic step-section analysis. 2005;46(10):1642-1649. Available at: <https://www.scopus.com/record/display.uri?eid=2-s2.0-33644673784&origin=inward&txGid=65d5fc85f3fb55c9b8d1565bf576bd47>. Accessed February 25, 2018.
- Evangelista L, Briganti A, Fanti S et al. New clinical indications for  $^{18}\text{F}$ /11C-choline, new tracers for positron emission tomography and a promising hybrid device for prostate cancer staging: a systematic review of the literature. *Eur Urol* 2016;70(1):161-175.
- Fanti S, Minozzi S, Castellucci P et al. PET/CT with  $^{11}\text{C}$ -choline for evaluation of prostate cancer patients with biochemical recurrence: meta-analysis and critical review of available data. *Eur J Nucl Med Mol Imaging* 2016;43(1):55-69.

24. Ceci F, Herrmann K, Castellucci P et al. Impact of <sup>11</sup>C-choline PET/CT on clinical decision making in recurrent prostate cancer: results from a retrospective two-centre trial. *Eur J Nucl Med Mol Imaging* 2014;41(12):2222-2231.
25. Castellucci P, Fuccio C, Nanni C et al. Influence of trigger PSA and PSA kinetics on <sup>11</sup>C-choline PET/CT detection rate in patients with biochemical relapse after radical prostatectomy. *J Nucl Med* 2009;50(9):1394-1400.
26. Lee MS, Cho JY, Kim SY et al. Diagnostic value of integrated PET/MRI for detection and localization of prostate cancer: Comparative study of multiparametric MRI and PET/CT. *J Magn Reson Imaging* 2017;45(2):597-609.
27. Kim Y il, Cheon GJ, Paeng JC et al. Usefulness of MRI-assisted metabolic volumetric parameters provided by simultaneous <sup>18</sup>F-fluorocholine PET/MRI for primary prostate cancer characterization. *Eur J Nucl Med Mol Imaging* 2015;42(8):1247-1256.
28. Jager PL, Vaalburg W, Pruim J, de Vries EG, Langen KJ, Piers DA. Radiolabeled amino acids: basic aspects and clinical applications in oncology. *J Nucl Med* 2001;42(3):432-445.
29. Schuster DM, Nieh PT, Jani AB et al. Anti-3-<sup>18</sup>F-FACBC positron emission tomography-computerized tomography and <sup>111</sup>In-capromab pendetide single photon emission computerized tomography-computerized tomography for recurrent prostate carcinoma: results of a prospective clinical trial. *J Urol* 2014;191(5):1446-1453.
30. Nanni C, Zanoni L, Pultrone C et al. <sup>18</sup>F-FACBC (anti-1-amino-3-<sup>18</sup>F-fluorocyclobutane-1-carboxylic acid) versus <sup>11</sup>C-choline PET/CT in prostate cancer relapse: results of a prospective trial. *Eur J Nucl Med Mol Imaging* 2016;43(9):1601-1610.
31. Turkbey B, Mena E, Shih J et al. Localized prostate cancer detection with <sup>18</sup>F FACBC PET/CT: comparison with MR imaging and histopathologic analysis. *Radiology* 2014;270(3):849-856.
32. Suzuki H, Inoue Y, Fujimoto H et al. Diagnostic performance and safety of NMK36 (trans-1-amino-3-[<sup>18</sup>F]fluorocyclobutanecarboxylic acid)-PET/CT in primary prostate cancer: multicenter phase IIb clinical trial. *Jpn J Clin Oncol* 2016;46(2):152-162.
33. Wright GL, Haley C, Beckett M, Lou J et al. Expression of prostate-specific membrane antigen in normal, benign, and malignant prostate tissues. *Urol Oncol Semin Orig Investig* 1995;1(1):18-28.
34. Bouchelouche K, Turkbey B, Choyke PL. PSMA PET and radionuclide therapy in prostate cancer. *Semin Nucl Med* 2016;46(6):522-535.
35. Demirci E, Sahin OE, Ocak M et al. Normal distribution pattern and physiological variants of <sup>68</sup>Ga-PSMA-11 PET/CT imaging. *Nucl Med Commun* 2016;37(11):1.
36. Perera M, Papa N, Christidis D et al. Sensitivity, specificity, and predictors of positive <sup>68</sup>Ga-prostate-specific membrane antigen positron emission tomography in advanced prostate cancer: a systematic review and meta-analysis. *Eur Urol* 2016;70(6):926-937.
37. Morigi JJ, Stricker PD, van Leeuwen PJ et al. Prospective comparison of <sup>18</sup>F-fluoromethylcholine versus <sup>68</sup>Ga-PSMA PET/CT in prostate cancer patients who have rising PSA after curative treatment and are being considered for targeted therapy. *J Nucl Med* 2015;56(8):1185-1190.
38. Freitag MT, Radtke JP, Afshar-Oromieh A et al. Local recurrence of prostate cancer after radical prostatectomy is at risk to be missed in <sup>68</sup>Ga-PSMA-<sup>11</sup>-PET of PET/CT and PET/MRI: comparison with mpMRI integrated in simultaneous PET/MRI. *Eur J Nucl Med Mol Imaging* 2017;44(5):776-787.
39. Maurer T, Gschwend JE, Rauscher I et al. Diagnostic efficacy of <sup>68</sup>Gallium-PSMA positron emission tomography compared to conventional imaging for lymph node staging of 130 consecutive patients with intermediate to high risk prostate cancer. *J Urol* 2016;195(5):1436-1443.
40. Eiber M, Herrmann K, Calais J et al. Prostate cancer molecular imaging standardized evaluation (PROMISE): proposed mTNM classification for the interpretation of PSMA-ligand PET/CT. *J Nucl Med* 2018;59(3):469-478.
41. Eiber M, Nekolla SG, Maurer T, Weirich G, Wester HJ, Schwaiger M. <sup>68</sup>Ga-PSMA PET/MR with multimodality image analysis for primary prostate cancer. *Abdom Imaging* 2015;40(6):1769-1771.
42. Search of: PET | recruiting, not yet recruiting, active, not recruiting, enrolling by invitation | Prostate Cancer | United States - List Results - ClinicalTrials.gov. Available at: <https://clinicaltrials.gov>. Accessed September 14, 2017.
43. Holland JP, Divilov V, Bander NH et al. <sup>89</sup>Zr-DFO-J591 for immunoPET of prostate-specific membrane antigen expression in vivo. *J Nucl Med* 2010;51:1293-1300.
44. Pandit-Taskar N, O'Donoghue JA, Ruan S et al. First-in-human imaging with <sup>89</sup>Zr-Df-IAB2M anti-PSMA minibody in patients with metastatic prostate cancer: pharmacokinetics, biodistribution, dosimetry, and lesion uptake. *J Nucl Med* 2016;57(12):1858-1864.
45. Beattie BJ, Smith-Jones PM, Jhanwar YS et al. Pharmacokinetic assessment of the uptake of 16-<sup>18</sup>F-fluoro-5-dihydrotestosterone (FDHT) in prostate tumors as measured by PET. *J Nucl Med* 2010;51(2):183-192.
46. Pandit-Taskar N, Veach DR, Fox JJ, Scher HI, Morris MJ, Larson SM. Evaluation of castration-resistant prostate cancer with androgen receptor-axis imaging. *J Nucl Med* 2016;57(Suppl 3):73S-78S.
47. Schuster DM, Nanni C, Fanti S. Evaluation of prostate cancer with radiolabeled amino acid analogs. *J Nucl Med* 2016;57(Suppl 3):61S-66S.
48. Pierr M, Shao X, Raffel D et al. Preclinical evaluation of <sup>11</sup>C-sarcosine as a substrate of proton-coupled amino acid transporters and first human application in prostate cancer. *J Nucl Med* 2017;58(8):1216-1223.
49. Spick C, Herrmann K, Czernin J. Evaluation of prostate cancer with <sup>11</sup>C-acetate PET/CT. *J Nucl Med* 2016;57(Suppl 3):30S-37S.
50. Buchegger F, Garibotto V, Zilli T et al. First imaging results of an intraindividual comparison of <sup>11</sup>C-acetate and <sup>18</sup>F-fluorocholine PET/CT in patients with prostate cancer at early biochemical first or second relapse after prostatectomy or radiotherapy. *Eur J Nucl Med Mol Imaging* 2014;41(1):68-78.
51. Yoshii Y, Furukawa T, Oyama N et al. Fatty acid synthase is a key target in multiple essential tumor functions of prostate cancer: uptake of radiolabeled acetate as a predictor of the targeted therapy outcome. *PLoS One* 2013;8(5):e64570.
52. Mansi R, Minamimoto R, Macke H, Jagaru AH. Bombesin-targeted PET of prostate cancer. *J Nucl Med* 2016;57(Suppl 3):67S-72S.
53. Lopci E, Grassi I, Chiti A et al. PET radiopharmaceuticals for imaging of tumor hypoxia: a review of the evidence. *Am J Nucl Med Mol Imaging* 2014;4(4):365-384.
54. Garcia-Parra R, Wood D, Shah RB et al. Investigation on tumor hypoxia in resectable primary prostate cancer as demonstrated by <sup>18</sup>F-FAZA PET/CT utilizing multimodality fusion techniques. *Eur J Nucl Med Mol Imaging* 2011;38(10):1816-1823.
55. Tehrani OS, Shields AF. PET imaging of proliferation with pyrimidines. *J Nucl Med* 2013;54(6):903-912.
56. Jadvar H. Imaging cellular proliferation in prostate cancer with positron emission tomography. *Asia Ocean J Nucl Med Biol* 2015;3(2):72-76.
57. Sun H, Sloan A, Mangner TJ et al. Imaging DNA synthesis with [<sup>18</sup>F]FMAU and positron emission tomography in patients with cancer. *Eur J Nucl Med Mol Imaging* 2005;32(1):15-22.
58. Tripathi S, Trabulsi EJ, Gomella L et al. VPAC1 targeted <sup>64</sup>Cu-TP3805 positron emission tomography imaging of prostate cancer: preliminary evaluation in man. *Urology* 2016;88:111-118.
59. Doran MG, Watson PA, Cheal SM et al. Annotating STEAP1 regulation in prostate cancer with <sup>89</sup>Zr immuno-PET. *J Nucl Med* 2014;55(12):2045-2049.
60. Persson M, Skovgaard D, Brandt-Larsen M et al. First-in-human uPAR PET: imaging of cancer aggressiveness. *Theranostics* 2015;5(12):1303-1316.